

Electrokinetic Flow Velocity in Charged Slit-like Microfluidic Channels with Linearized Poisson-Boltzmann Field

Myung-Suk Chun[†]

Complex Fluids and Membrane Team, Korea Institute of Science and Technology (KIST),
PO Box 131, Cheongryang, Seoul 130-650, South Korea
(Received 6 May 2002 • accepted 25 June 2002)

Abstract—In cases of the microfluidic channel, where the thickness of electric double layer is often comparable with the characteristic size of flow channels, the electrokinetic influence on the flow behavior can be found. The externally applied body force originating from the electrostatic interaction between the linearized Poisson-Boltzmann field and the flow-induced electrical field is applied in the equation of motion. An analytical solution to this Navier-Stokes equation of motion for well-defined geometry of slit-like microchannel is obtained by employing Green's function. Also, an explicit analytical expression for the induced electrokinetic potential is successfully derived as functions of relevant physicochemical parameters. The effects of the ionic concentration of the fluid, the zeta potential of the solid surface, and the width of microchannels on the velocity profile as well as the streaming potential are examined. The electric double layer effect on the velocity profile becomes stronger as the channel width decreases, where the average fluid velocity is entirely reduced with the decrease in ionic concentration. The induced electrokinetic potential increases with an increase in pressure gradient, while it decreases as the ionic concentration increases.

Key words: Electrokinetic Flow, Electrostatic Interaction, Microfluidic Channel, Navier-Stokes Equation, Poisson-Boltzmann Equation

INTRODUCTION

When a charged surface is in contact with an electrolyte, the electrostatic charges on the solid surface will influence the distribution of nearby ions in the electrolyte solution. Then an electric field is established, where the charges on the solid surface and the balancing charges in the liquid is called the Debye electric double layer. The inner boundary of double layer is referred to as the Stern layer, and the ions located beyond the Stern plane form the shear plane as well as the diffuse mobile part of the double layer. Electrokinetics refers to those processes in which the boundary layer between one charged phase and another is forced to undergo some sort of shearing process. The charge attached to solid will then move in one direction and that associated with the adjoining phase will move in the opposite direction. The no-slip fluid flow boundary condition is assumed on the shear plane, and the potential at this plane is referred to as the electrokinetic potential, more commonly known as the zeta potential [Russel et al., 1989].

The electrokinetic principle is closely related to electroosmosis, electrophoresis, and streaming potential phenomena. Further, an understanding of the fundamental behavior of the fluid flow in microchannels is of considerable importance in the research fields of micro- and nanofluidics. Microchannels currently have wide applications in the design and utilization of microfluidic devices, such as diagnostic microdevices, biomedical microchips, microreactors, and other MEMS (micro-electro mechanical system) devices [Manz et al., 1994; Hu et al., 1999]. It should be noted that laminar flow is the definitive characteristic of microfluidics. Fluid flowing in micro-

channels with dimensions on the order of tens or hundreds of micrometers and at readily achievable flow speeds is characterized by low Reynolds number [Stone and Kim, 2001]. Pressure-driven motion, termed Poiseuille flow, is well understood, but the fluid flow behavior in charged microchannels is influenced by the electrokinetic effect and hence deviates from that described by the traditional form of the Navier-Stokes equation.

Earlier studies dealing with electrokinetic flow in cylindrical channels can be favorably found. The effect of the surface potential on fluid transport through narrow cylindrical capillary with the Debye-Hückel approximation was discussed [Rice and Whitehead, 1965]. Later, the same problem with higher surface potential was investigated by developing an approximate solution to the Poisson-Boltzmann (P-B) equation pertaining to an imposed electric field [Levine et al., 1975]. In this study, the electrokinetic flow behavior in a slit-like channel is analyzed by employing the Green's function formulation. The electrostatic potential is firstly considered by solving the linearized P-B equation, and then the equation of motion is developed by dealing with the external body force and the relevant flow-induced electrical field. The velocity profile is predicted with variations of channel width, Debye layer thickness, and zeta potential of the channel wall.

ELECTRIC FIELD IN A CHARGED MICROCHANNEL

The P-B equation is a mean-field approximation in that the positions of the individual ions in solution are replaced by the mean concentration of ions. The nonlinear P-B equation governing the electric field is given as

$$\nabla^2 \Psi = \kappa^2 \sinh \Psi. \quad (1)$$

[†]To whom correspondence should be addressed.
E-mail: mschun@kist.re.kr

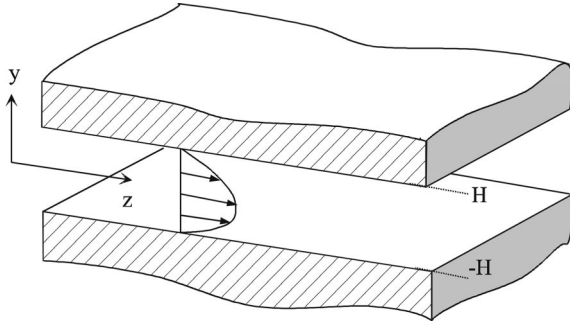


Fig. 1. A fluid flow within charged slit-like microchannel.

Here, the dimensionless potential Ψ denotes $z_i e \psi / kT$ and the inverse Debye double layer thickness κ is defined by

$$\kappa = \left[\frac{2n_{i,b} z_i^2 e^2}{\epsilon kT} \right]^{1/2} \quad (2)$$

where $n_{i,b}$ is the concentration of type i ions in the bulk solution, z_i the valence of type i ions, e the elementary charge, ϵ the dielectric constant, and kT the Boltzmann thermal energy. For low potential of $\Psi \leq 1$ (i.e., less than $kT/e = 25.69$ mV) with 1 : 1 electrolyte system, the P-B equation may be linearized. This linearized version is called the Debye-Hückel equation [Russel et al., 1989].

We consider a slit-like channel confined between parallel planes of width $2H$ as shown in Fig. 1, then the linearized P-B equation leads to

$$\frac{\partial^2 \Psi}{\partial y^2} = \kappa^2 \Psi. \quad (3)$$

The following boundary conditions are presented in a half of the slit cross section,

$$\Psi = \Psi_s \quad \text{at } y=H, \quad (4a)$$

$$\frac{d\Psi}{dy} = 0 \quad \text{at } y=0. \quad (4b)$$

The solution to Eq. (3) can be obtained with these boundary conditions, which is derived as

$$\Psi = \Psi_s \frac{\cosh \kappa y}{\cosh \kappa H}. \quad (5)$$

From Eq. (5), it is straightforward to determine the local net charge density as follows

$$\rho_e = z_i e (n_+ - n_-) = -2z_i e n_{i,b} \sinh \Psi. \quad (6)$$

FLOW FIELD COUPLED WITH ELECTROKINETIC INTERACTION

1. Flow through a Charged Slit-like Channel

In principle, the Navier-Stokes equation furnishes the paradigm for describing the equation of motion for an incompressible ionic fluid, given by

$$\rho \frac{\partial \mathbf{v}}{\partial t} + \rho (\mathbf{v} \cdot \nabla) \mathbf{v} = -\nabla p + \mathbf{F} + \eta \nabla^2 \mathbf{v} \quad (7)$$

where ρ and η are the density and viscosity of the fluid, respec-

tively. Let us consider the one-dimensional laminar flow through a slit-like channel, then $\mathbf{v} = [0, 0, v_z(y)]$ is taken with Cartesian coordinates [Happel and Brenner, 1983]. Neglecting gravitational forces, the body force per unit volume \mathbf{F} ubiquitously caused by the z -directional action of an induced electrical field E_z on the net charge density ρ_e can be written $F_z = \rho_e E_z$. With these identities, Eq. (7) is reduced to

$$\eta \frac{d^2 v}{dy^2} = \frac{dp}{dz} - \rho_e E_z. \quad (8)$$

In view of taking a flow only in the z -direction in a slit spaced a distance $2H$ apart, the velocity profile known as a plane Poiseuille flow is obtained as

$$v_z = \frac{H^2}{2\eta} \frac{dp}{dz} \left[1 - \left(\frac{y}{H} \right)^2 \right]. \quad (9)$$

One obtains the nondimensionalized equation of motion, such that

$$\frac{d^2 V}{dY^2} = \frac{dP}{dZ} + \Gamma_1 E \Psi \quad (10)$$

with the following dimensionless parameters

$$\begin{aligned} Z &= \frac{z}{d_h \text{Re}}, \quad Y = \frac{y}{d_h}, \quad V = \frac{v}{U}, \quad \text{Re} = \frac{\rho d_h U}{\eta}, \\ P &= \frac{p}{\rho U^2}, \quad E = \frac{E_z d_h \text{Re}}{\Psi_0}, \quad \Gamma_1 = \frac{2z_i e n_{i,b} \Psi_0}{\rho U^2} \end{aligned} \quad (11)$$

where d_h means the hydraulic diameter (i.e., $4H$), U the reference velocity, and Ψ_0 the reference electrical potential. The boundary conditions are applied as

$$V = 0 \quad \text{at } Y = \frac{H}{d_h}, \quad (12a)$$

$$\frac{dV}{dY} = 0 \quad \text{at } Y = 0. \quad (12b)$$

The Green's function formulation with the differential operator \mathcal{L} , which is described in the reference books [see, e.g., Arfken, 1985], can be used for $V(Y, t)$ as follows:

$$\mathcal{L}V = \left[\eta \frac{\partial}{\partial t} - \frac{\partial^2}{\partial Y^2} \right] V = -\frac{\partial P}{\partial Z} - E \Gamma_1 \Psi(Y). \quad (13)$$

Solution of this equation proceeds by standard techniques. We here consider Green's function as a linear combination of the eigenvalues and corresponding eigenfunctions ϕ_n , established as

$$G(Y, Y', t) = \sum_n e^{-\beta_n t} \phi_n(Y) \phi_n(Y') \quad (14)$$

where t is normalized by $\rho d_h^2 / \eta$, and a convenient representation for the eigenvalues

$$\beta_n = \left[\frac{(2n-1)\pi d_h}{2H} \right]^2. \quad (15)$$

Utilization of the Dirac delta function with orthogonal properties leads to the following expression

$$\mathcal{L}G(Y, Y', t) \equiv \delta(Y - Y') \delta(t). \quad (16)$$

Then, the solution of Eq. (13) subjected to the above boundary con-

ditions is given by

$$V(Y, t) = \int_0^t dt' \int_0^{H/d_h} dY' G(Y, Y', t-t') \left[-\frac{dP}{dZ} - E\Gamma_1 \Psi(Y') \right]. \quad (17)$$

Green's function is explicitly found by using the separation of variables method, yielding

$$G = \frac{d_h}{H} \sum_{n=1}^{\infty} e^{-\frac{(2n-1)^2 \pi^2 d_h^2}{4H^2} t'} \cos \frac{(2n-1)\pi d_h}{2H} Y \cos \frac{(2n-1)\pi d_h}{2H} Y'. \quad (18)$$

The solution for velocity profile yields as

$$\begin{aligned} V(Y, t) &= \frac{d_h}{H} \sum_{n=1}^{\infty} \lim_{t' \rightarrow \infty} \int_0^t dt' e^{-\beta_n(t-t')} \int_{-H/d_h}^{H/d_h} dY' \cos \sqrt{\beta_n} Y \cos \sqrt{\beta_n} Y' \\ &\quad \times \left[-\frac{dP}{dZ} - E\Gamma_1 \Psi(Y') \right] \\ &= \frac{d_h}{H} \sum_{n=1}^{\infty} \lim_{t' \rightarrow \infty} \int_0^t dt' e^{-\beta_n(t-t')} \int_{-H/d_h}^{H/d_h} dY' \cos \sqrt{\beta_n} Y \cos \sqrt{\beta_n} Y' \\ &\quad \times \left[-\frac{dP}{dZ} - E\Gamma_1 \Psi \left(\frac{\cosh \kappa d_h Y'}{\cosh \kappa H} \right) \right]. \end{aligned} \quad (19)$$

Both integrating and rearranging give the velocity profile as follows,

$$\begin{aligned} V(Y) &= \frac{2d_h}{H} \sum_{n=1}^{\infty} \frac{(-1)^n}{\beta_n^{3/2}} \cos \sqrt{\beta_n} Y \left[\frac{dP}{dZ} + \frac{\beta_n E \Gamma_1 \Psi_s}{(\kappa d_h)^2 + \beta_n} \right] \\ &= V_{inert}(Y) + \frac{2d_h}{H} \sum_{n=1}^{\infty} \frac{(-1)^n}{\beta_n^{1/2}} \cos \sqrt{\beta_n} Y \left(\frac{E \Gamma_1 \Psi_s}{(\kappa d_h)^2 + \beta_n} \right). \end{aligned} \quad (20)$$

where V_{inert} is the velocity profile in the absence of the electrostatic interaction, that equals to the plane Poiseuille flow profile given in Eq. (9). Ultimately, the average fluid velocity is obtained as

$$\begin{aligned} \langle V \rangle &= \frac{\int_0^{H/d_h} V dY}{\int_0^{H/d_h} dY} = -\frac{2d_h^2}{H^2} \sum_{n=1}^{\infty} \frac{1}{\beta_n^2} \left[\frac{dP}{dZ} + \frac{\beta_n E \Gamma_1 \Psi_s}{(\kappa d_h)^2 + \beta_n} \right] \\ &= -\langle V_{inert} \rangle - \frac{2d_h^2}{H^2} E \Gamma_1 \Psi_s \sum_{n=1}^{\infty} \frac{1}{\beta_n ((\kappa d_h)^2 + \beta_n)}. \end{aligned} \quad (21)$$

2. Flow-induced Electrokinetic Potential (Streaming Potential)

As derived in Eq. (10), both the local velocity and the average fluid velocity can be calculated when the nondimensional induced electrical field E is known. Ions from the double layer region are transported along with the streaming solution, resulting in a streaming current I_s , in the direction of flow. The resultant induced electrokinetic potential, which is generally called the streaming potential E_s , then induces a flow of ions in the opposite direction known as the electrical conduction current I_c . When the flow reaches a steady state, the summation of the streaming and conduction current should be zero, so that

$$\nabla \cdot I = I_s + I_c = 0. \quad (22)$$

The streaming current I_s caused by the pressure-driven liquid flow is called the electrical convection current. For a slit-like microchannel with the specified width W , it is defined by

$$\begin{aligned} I_s &= W d_h U \int dY \rho_c V \\ &= \frac{4W d_h^2 U \epsilon \kappa^2 \Psi_s}{H} \sum_{n=1}^{\infty} \frac{1}{\beta_n ((\kappa d_h)^2 + \beta_n)} \left[\frac{dP}{dZ} + \frac{\beta_n E \Gamma_1 \Psi_s}{(\kappa d_h)^2 + \beta_n} \right]. \end{aligned} \quad (23)$$

The electrical conduction current I_c can be expressed as

$$I_c = \lambda_c E A_c = \lambda_c \frac{E_s \Psi_o}{d_h \text{Re}} 2HW \quad (24)$$

where λ_c is the total electrical conductivity and A_c is the cross-sectional area of the channel. Note that the electrical conduction current consists of bulk electrical conductivity and surface electrical conductivity. The bulk conductivity of the monovalent symmetric electrolyte system (e.g., NaCl, KCl solution) is almost much greater than the surface conductivity of the channels made on inorganic or polymeric materials [Lee et al., 2000]. In this respect, the λ_c in this study can be determined by the value of the bulk conductivity. Substituting Eqs. (23) and (24) into Eq. (22), the nondimensional induced electrokinetic potential E is derived as

$$E = \frac{d_h^2 U \text{Re} \int_{-H/d_h}^{H/d_h} dY \left(\epsilon \kappa^2 \Psi_s \frac{\cosh \kappa d_h Y}{\cosh \kappa H} \right) V_{inert}}{1 + \frac{2d_h^3 U \Gamma_1 \text{Re} \Psi_s^2 \epsilon \kappa^2}{H^2 \lambda_c \Psi_o} \sum_{n=1}^{\infty} \frac{1}{((\kappa d_h)^2 + \beta_n)^2}}. \quad (25)$$

With defining the dimensionless variable $\Gamma_2 = 2Z_e n_b d_h U / \lambda_c \Psi_o$, Eq. (25) can be finally expressed as follows,

$$E = -\frac{\frac{2d_h^2 \Gamma_2 \text{Re} \Psi_s}{H^2} \sum_{n=1}^{\infty} \frac{1}{((\kappa d_h)^2 + \beta_n)} \left(\frac{dP}{dZ} \right)}{1 + \frac{2d_h^2 \Gamma_1 \Gamma_2 \text{Re} \Psi_s^2}{H^2} \sum_{n=1}^{\infty} \frac{1}{((\kappa d_h)^2 + \beta_n)^2}}. \quad (26)$$

RESULTS

Illustrative computations are performed by considering a fully developed laminar flow of an aqueous NaCl solution through a slit-like microchannel made on inorganic materials such as fused silica. At room temperature, the dielectric constant and the viscosity of the fluid can be taken as $\epsilon = (80) \times (8.854 \times 10^{-12})$ Coul/N·m² and $\eta = 1 \times 10^{-3}$ kg/m·sec, in respect. From the applied pressure gradient dp/dz , the reference velocity U is estimated as $(H^2/4\eta)(dp/dz)$. Both the double layer thickness and the bulk conductivity with variations of ionic concentrations are provided in Table 1, where the bulk conductivity is chosen from the literature value [Lide, 1999]. For 1 : 1 type of NaCl electrolyte, the ionic concentration equals the ionic strength of the solution.

Eq. (20) is an exact solution to the equation of motion by applying Green's function. In Figs. 2-4, the velocity profiles are plotted with variations of electrostatic repulsion, for which both the Debye double

Table 1. The condition of NaCl aqueous solution environment

Ionic strength, ¹⁾ C_b (mM)	Double layer thickness, ²⁾ κ^{-1} (nm)	Bulk conductivity (1/Ω·m)
10	3.1	1.2×10^{-1}
10	9.7	1.2×10^{-2}
10^{-2}	96.5	1.6×10^{-4}
10^{-4}	964.7	1.8×10^{-6}

¹⁾ $n_{i,b}$ (1/m³) = $N_A [C_b$ (mM)], where N_A is Avogadro's number.

²⁾for 1 : 1 type electrolytes, Double layer thickness (nm) = $[C_b$ (M)]^{-1/2} / 3.278.

layer thickness and surface potentials are changed. It is possible to assume here that the surface potential Ψ_s is identical to the zeta potential. This points out that the flow situations are verified as a low Reynolds number condition, which is certainly less than 1. A decrease of NaCl electrolyte concentration C_b corresponds to an increase of Debye double layer thickness κ^{-1} . The ionic strength of 10^{-4} mM nearly satisfies to the range for distilled water. As shown

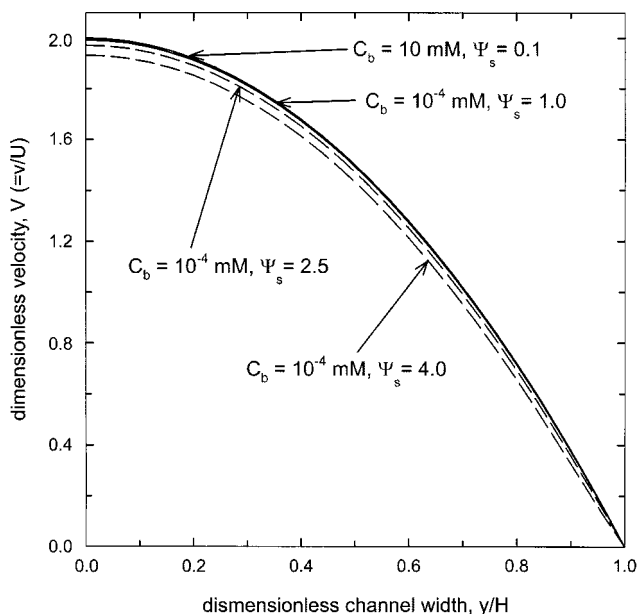


Fig. 2. Velocity profile in a slit-like microchannel with channel width $2H=30\ \mu\text{m}$ for several Debye double layer thickness as well as surface potentials, where pressure gradient dp/dz is $2.026 \times 10^5\ \text{N/m}^3$.

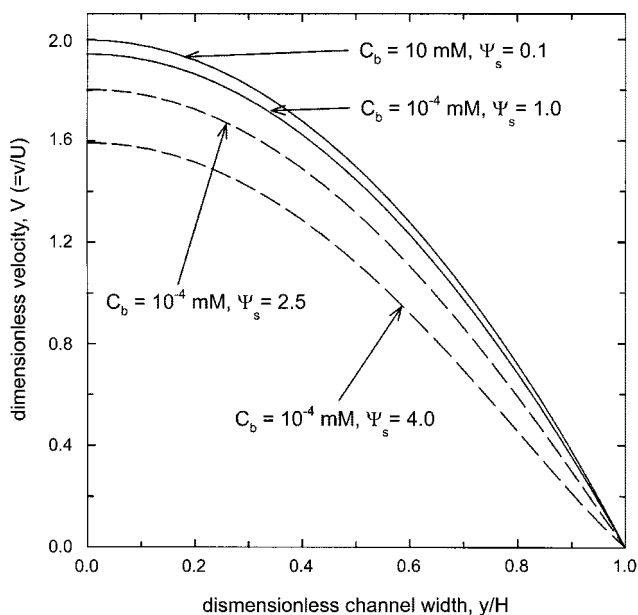


Fig. 3. Velocity profile in a slit-like microchannel with channel width $2H=10\ \mu\text{m}$ for several Debye double layer thickness as well as surface potentials, where pressure gradient dp/dz is $2.026 \times 10^5\ \text{N/m}^3$.

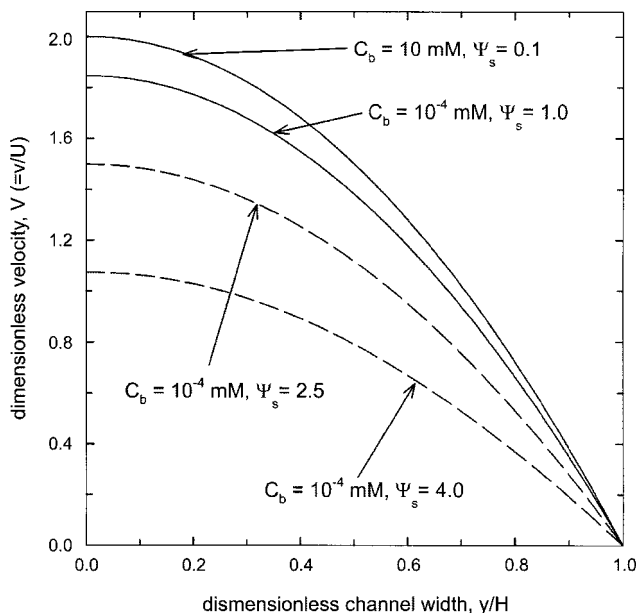


Fig. 4. Velocity profile in a slit-like microchannel with channel width $2H=2\ \mu\text{m}$ for several Debye double layer thickness as well as surface potentials, where pressure gradient dp/dz is $2.026 \times 10^5\ \text{N/m}^3$.

in Fig. 2, the Debye electric double layer exhibits weak effects on the flow pattern for the channel width of $30\ \mu\text{m}$. The dashed curves obtained with dimensional surface potentials above $25.69\ \text{mV}$ (i.e., $\Psi_s=2.5$ and 4.0) are hypothetical predictions, since the present study deals with the linearized P-B field provided in Eq. (5). However, these dashed curves show a strong dependency of the surface potential upon the velocity profile, although they are not necessarily true.

As demonstrated in Figs. 3 and 4, it is obvious that the double layer effect on the flow pattern becomes stronger as the channel width decreases. The maximum velocity in the center of the channel is much lower than that in the original Poiseuille flow, with increasing of the electrostatic interaction. It is shown that as the surface potential increases the flow velocity near the channel wall approaches zero due to the action of the electric double layer field and the induced electrokinetic potential.

As described before, the charge concentration difference between the upstream and the downstream results in an induced electrokinetic potential E_s , namely streaming potential. Therefore, a larger pressure gradient will generate a larger volume transport, and as displayed in Fig. 5, a higher charge accumulation as well as a stronger induced electrical field will occur. Fig. 5 also shows that the induced electrical field increases as the ionic concentration of the aqueous solution for a given pressure gradient decreases, due to a larger double layer thickness. In Fig. 6, on the other hand, the average fluid velocity $\langle v \rangle$ is entirely reduced with the decrease in ionic concentration. This behavior leads us to understand the electrokinetic effect in the fluid flow through microchannels.

The predicted results indicate the fact that the velocity profiles dramatically change when the microchannel wall is charged with higher surface potentials. Therefore, the behavior of electrokinetic flows with respect to the full P-B field needs to be elucidated, and

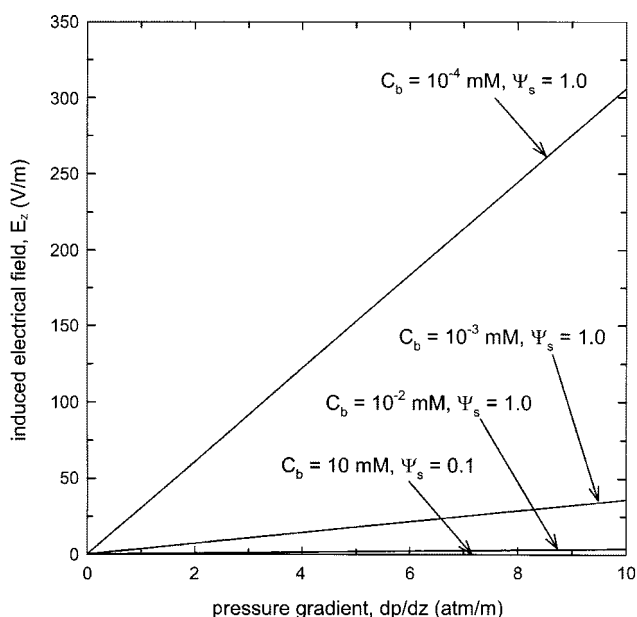


Fig. 5. The variations of induced electrical field E_z with pressure gradient at different solution ionic concentrations as well as surface potentials, where the channel width $2H$ is $10\ \mu\text{m}$.

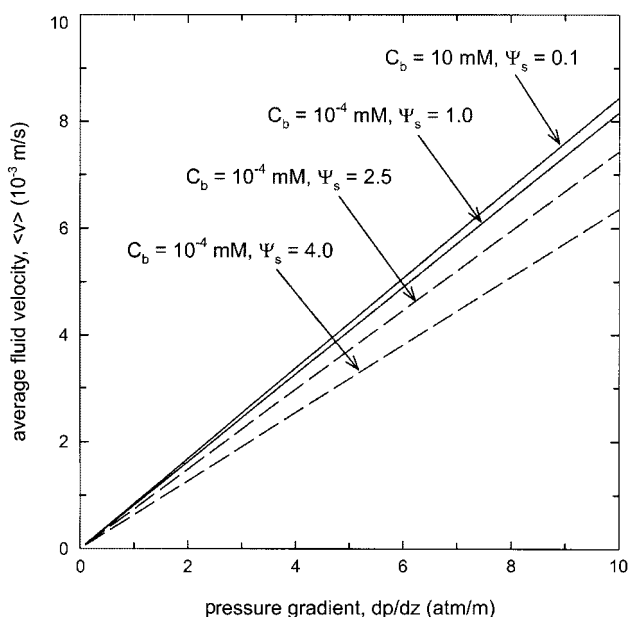


Fig. 6. The variations of average fluid velocity $\langle v \rangle$ with pressure gradient at different solution ionic concentrations as well as surface potentials, where the channel width $2H$ is $10\ \mu\text{m}$.

a fortiori, this problem should be analyzed in future study.

CONCLUSIONS

Although earlier studies exist for electrokinetic flow in cylindrical channels, microchannel analysis of the requisite microfluidic problems has not been confronted until recently. The main thrust of the present study is an analysis on the electrokinetic flow of ionic fluids in slit-like microchannels. The additional body force origi-

nating from the presence of the electric field and the flow-induced electrical field was considered in the equation of motion. Applying Green's function formula could derive the expressions in explicit forms for the velocity profile, the induced electrokinetic potential, and the average fluid velocity as functions of relevant parameters.

Theoretical results emphasize that the velocity profile is clearly affected by the Debye double layer for the cases of low ionic concentrations and high zeta potentials. The induced electrokinetic potential increases with the pressure gradient, while it decreases as the ionic concentration increases. Since both the electric double layer and the induced electrokinetic potential act against the liquid flow, they result in a reduced flow rate and this behavior is related to the electroviscous effect. Further studies are needed to explore with regard to corresponding behavior for the nonlinear P-B field.

ACKNOWLEDGEMENT

This work was supported by the Specified Basic Research Fund (Grant No. R01-2001-000-00411-0) from the Korea Science and Engineering Foundations (KOSEF).

NOMENCLATURE

- A_c : cross-sectional area of the channel [m^2]
- C_b : solution ionic strength [M]
- d_h : hydraulic diameter [m]
- E : dimensionless induced electrokinetic potential, or streaming potential [-]
- E_z : dimensional E [V/m]
- e : elementary charge [Coul]
- F : body force [N/m^3]
- G : Green's function [-]
- H : half channel width [m]
- I : net electrical current [A]
- I_c : electrical conduction current [A]
- I_s : electrical convection current [A]
- kT : Boltzmann thermal energy [J]
- N_A : Avogadro's number
- $n_{i,b}$: concentration of charged ions [$1/\text{m}^3$]
- P : dimensionless hydraulic pressure [-]
- p : hydraulic pressure [N/m^2]
- Re : Reynolds number [-]
- t : dimensionless time [-]
- U : reference velocity [m/s]
- V : dimensionless fluid velocity [-]
- $\langle V \rangle$: dimensionless average fluid velocity [-]
- v : fluid velocity component [m/s]
- W : specified channel width [m]
- Y : non-dimensional y-coordinate [-]
- Z : non-dimensional z-coordinate [-]
- z_i : valence of ion [-]

Greek Letters

- β_n : set of eigenvalues [-]
- ϵ : dielectric constant [$\text{Coul}^2/\text{J}\cdot\text{m}$]
- ϕ_n : set of eigenfunctions [-]
- κ : inverse Debye double layer thickness [$1/\text{m}$]

- ρ : fluid density [kg/m³]
 ρ_e : net charge density [Coul/m³]
 η : fluid viscosity [kg/m·s]
 Γ_1, Γ_2 : non-dimensional parameters [-]
 λ_e : total electrical conductivity [1/Ω·m]
 Ψ : dimensionless electrostatic potential [-]
 Ψ_s : dimensionless electrostatic surface potential [-]
 Ψ_o : reference electrical potential [V]

REFERENCES

- Arfken, G., "Mathematical Methods for Physicists," 3rd Ed., Academic Press, New York (1985).
- Happel, J. and Brenner, H., "Low Reynolds Number Hydrodynamics: with Special Applications to Particulate Media," Martinus Nijhoff, Hague (1983).
- Hu, L., Harrison, D. J. and Masliyah, J. H., "Numerical Model of Electrokinetic Flow for Capillary Electrophoresis," *J. Colloid Interface Sci.*, **215**, 300 (1999).
- Lee, S.-Y., Chun, M.-S. and Kim, J.-J., "The Behavior of Membrane Potential Changes During Filtration of Latex Colloids," *HWAHAK KONGHAK*, **38**, 173 (2000).
- Levine, S., Marriott, J. R., Neale, G. and Epstein, N., "Theory of Electrokinetic Flow in Fine Cylindrical Capillaries at High Zeta-Potentials," *J. Colloid Interface Sci.*, **52**, 136 (1975).
- Lide, D. R. (Eds.), "CRC Handbook of Chemistry and Physics," 80th Ed., CRC Press, FL (1999).
- Manz, A., Effenhauser, C. S., Burggraf, N., Harrison, D. J., Seller, K. and Flurl, K., "Electroosmotic Pumping and Electrophoretic Separations for Miniaturized Chemical Analysis Systems," *J. Micromech. Microeng.*, **4**, 257 (1994).
- Rice, C. L. and Whitehead, R., "Electrokinetic Flow in a Narrow Cylindrical Capillary," *J. Phys. Chem.*, **69**, 4017 (1965).
- Russel, W. B., Saville, D. A. and Schowalter, W. R., "Colloidal Dispersions," Cambridge Univ. Press, New York (1989).
- Stone, H. A. and Kim, S., "Microfluidics: Basic Issues, Applications, and Challenges," *AIChE J.*, **47**, 1250 (2001).